RSC Advances

PAPER

View Article Online
View Journal | View Issue

Cite this: *RSC Adv.*, 2022, **12**, 29928

Flame-retardant effect of tannic acid-based intumescent fire-retardant applied on flammable natural rubber†

Jingchao Wang, ‡[a] Xueya Wang, ‡[a] Ziwen Zhou,[a] Xiaoyang Liu,[b] Meiming Xu,[b] Fa Zhao,[c] Feng Zhao, [a] Song Li, [a] Zhihua Liu, [a] Lin Li *[a] and Shuai Zhao*[a]

Tannic acid (TA) is a natural phenolic compound abundant in plants. Its characteristics of low combustion and good absorption make it useful in the flame retardant field. On this basis, a new expansive flame retardant system (ACT) composed of ammonium polyphosphate (APP)/TA functional clay (CT) was used to study the synergistic flame retardancy and smoke suppression of natural rubber (NR). Because of their unique flame retardancy and better mechanical properties compared with the traditional expansive flame retardant system (IFR), new flame retardants have attracted much attention in various fields. The results of the cone calorimeter showed that the ACT system can significantly influence the decomposition behavior of NR and form a highly graphitized and phosphorous carbon layer to protect the composite material, thus a synergistic effect is produced on the flame retardancy and smoke suppression performance of the composite material. In addition, within the effective additive quality range of the ACT system, TC can give the NR composite excellent mechanical properties.

Received 27th July 2022
Accepted 20th September 2022

DOI: 10.1039/d2ra04682b

rsc.li/rsc-advances

1 Introduction

In terms of environmental protection, expansion flame retardant (IFR) is a halogen-free flame retardant with broad benefits of antidroplet, low fire toxicity and low smoke.[1,2] Generally, IFR contains an acid source, a carbonizer and an air source.[3] In a fire, IFR produces an expansive, multi-cellular char layer that acts as a protecting barrier for the underlying material against heat transfer and oxygen diffusion, thereby preventing the pyrolysis of the material into volatile combustible compounds.[4] For traditional IFR, polyammonium phosphate (APP) is better than other flame retardants due to its low loading, low smoke, low cost and convenient processing technique.[5] However, compared with halogen-flame retardants, traditional APP has disadvantages such as strong moisture absorption and poor flame retardancy efficiency.[6–9] To solve these problems, people strive to study high-performance APP-based IFR systems.[10–13] While these achievements are impressive, APP-based IFR needs to be improved in terms of efficiency and environmental protection.[14,15] Clay minerals are abundant and cheap. It has important applications in the polymer flame retardation field due to its porous structure, big specific surface area and excellent absorbability.[16] Additionally, clay has prominent mechanical and thermal stability and is consistent with traditional processing performances (mixing, extrusion, molding, *etc.*).[17] In our previous work, TA was proposed to be used as a stabilizer and regulator for graphite water stripping to peel graphite from direct liquid phase into graphene.[18] TA, natural products are found mainly in pine bark, mimosa, and hemlock, as well as in the wood and tree ferns of some certain trees, which show some good properties, such as antioxidant effects,[19] inhibition,[20] antibacteria,[21] complexed with proteins,[22] and a reducing ability.[23] In addition, during a fire, TA can effectively reduce oxidants and free radicals, maximize unburned solids and char residues, and help the tree survive.[24]

In our previous work, TA functionalized graphene was combined with APP to design an efficient natural TA based expansive flame retardant system (AGT).[25] For AGT system, one important drawback is that graphene is less cost-effective. Inspired by the liquid-phase exfoliation technique of graphite into graphene using TA as stabilizer, in this study, the same lamellar structure and cost-effective clay replaces graphene to form a new intumescent flame retardant system (ACT). Each component has a dual identity, with such as APP as the acid source and gas source, TA as the acid source and carbonizer, and clay as the carbonizer and carbon layer enhancer. The effect of ACT on the flame retardant performance of rubber is studied in this paper. Rubber, especially rubber used as natural rubber,

[a]*Key Lab of Rubber-plastics, Ministry of Education/Shandong Provincial Key Lab of Rubber-plastics, School of Polymer Science and Engineering, Qingdao University of Science and Technology, Qingdao, 266042, China. E-mail: qustlilin@hotmail.com; lyzhsh@163.com*

[b]*Shandong Rike Chemical Co., Ltd, Changle, 262499, China*

[c]*Qingdao Haier Refrigerator Co., Ltd, China*

† Electronic supplementary information (ESI) available. See DOI: https://doi.org/10.1039/d2ra04682b

‡ These authors contributed equally to this work.

is an important industrial material, which is broadly used not only in automobile and industrial fields, but in aerospace parts.[26] However, it also has some weaknesses, especially the high fire risk. The loading of flame retardants can significantly influence flame retardancy of rubber materials. However, the flame-retardant effect is accompanied with negative effects, such as pollution of mechanical performances. Nevertheless, under the proper loading condition, the ACT expansion flame retardant can endow NR with flame retardant and reinforcement. The degradation process and combustion properties of ACT/NR composites are analyzed using thermogravimetric and combustion calorimetric analyses. The microstructure of char residues is examined using SEM and Raman. Based on the analysis of thermal decomposition behavior and carbon characteristics of polymer composites, the flame retardant mechanism is proposed.

2 Experimental and materials

2.1 Materials

Ammonium polyphosphate (APP, type is TF-201, the degree of polymerization is 1500) was generously supplied by Shandong Taifeng New Flame Retardant Co., Ltd (China). Clay was supplied by Weifang Lichuang New Materials Co., Ltd (China). Tannic acid (TA) was purchased from Aladdin Technology Co., Ltd (China). NR latex (solid content: 60 wt%) was provided by Weifang Lichuang New Materials Co., Ltd (China). Other reagents, including sulfur, *N*-cyclohexyl-2-benzothiazolesulfenamide (CZ), 2,2-dibenzothiazoledisulfide (DM), zinc oxide (ZnO), and N98 (98% SiO_2, average diameter: 200 nm) were all industrial grade and kindly supplied by Weifang Lichuang New Materials Co., Ltd (China).

2.2 Characterization

Raman spectroscopy is recorded using a high-resolution FRS-100S (Bruker) machine with a CCD detector which spectral purity is quoted to be <700 at wavelength >2100 cm^{-1} from a set wavelength. The infrared spectra were observed by Bruker Vertex 70 Fourier transform infrared spectrometer. The morphologies of the residual carbon layer were obtained using JSM-6700F SEM (Japan Electronics Corp.). TGA was measured using a TGA-7 thermal analyzer (PerkinElmer, USA). The heating rate was 10 °C min^{-1} at room temperature up to 800 °C in N_2 atmosphere. Dynamic mechanical analysis (DMA) was performed on a DMA242 machine (NETZSCH) with tensile mode and a 3 °C min^{-1} temperature increment. Limited oxygen index (LOI) was measured using the HC-2 oxygen Index meter (China Jiangning Analytical Instruments Co., Ltd) in accordance with standard ASTM D2863. UL-94 Vertical Burning Test was performed using a vertical burning instrument (CFZ-1 type, Jiangning Analysis Instrument Co., China) according to UL-94 test ASTM D3801-2010. The Cone Calorimeter Test (CCT) was performed on the cone calorimeter according to ASTM E1354/ISO 5660 (Fire Testing Technology, UK) under exposed an external heat flux of 35 kW m^{-2}. The thermal conductivity was recorded on a laser flash system (LFA 447 NanoFlash). Mechanical properties were carried out using an AI-7000S Universal Material Tester according to ISO 528:2009 with a dumbbell specimen at 500 mm min^{-1} tensile speed. According to ISO-4649 standard, wear test was carried out with DIN abrasive tool.

2.3 Preparation of TC

The variable clay is added to a vial containing 30 ml of TA solution, the concentration of clay is variable according to the batch composition shown in Table S1.† The mixture was then subjected to ultrasound (Elmasonic E30H, 40 W, 37 kHz) in a 30–35 °C water bath for 30 minutes to prepare TC.[18]

2.4 Preparation of the batches

A certain amount of TC aqueous dispersion (solidified into 5 mg mL^{-1}) was slowly added into NR latex under strong mechanical agitation. After adding 1 wt% sodium chloride solution to coagulated, the TC/NR compound was cut into small pieces and washed with distilled water to completely remove the sodium chloride. The TC/NR compound was then dried overnight in a vacuum oven at 60 °C. Mixing was carried out in a 200 ml banbury mixer at a rotation rate of 60 RPM at 120 °C. A certain amount of TC/NR mixer was added for premixing for 2 min, and then N98 (5PHr), ZnO (5PHR), APP (variable) and N330 (30 PHR) were successively added to mix for 8 min. And then the mixture was discharged onto a two roll mill at 40 °C, where the sulfur (1 phr), CZ (1.2 phr) and DM (0.6 phr) were added. The prepared composite material was labeled NR/ACT. The batch composition of NR/ACT system and ACT system were shown in Tables 1 and S1† respectively. For comparison, the NR/APP composite was prepared using APP and NR as reference samples (designed as NR/APP), and the same procedures were followed for the preparation of NR/ACT.

3 Results and discussion

3.1 Flame retardant properties of NR/APP and NR/ACT composites

The thermal combustion properties (LOI and UL-94) of NR/APP and NR/ACT were studied through experiment and theoretical analysis. The neat NR burns violently and drips down when it is ignited. As can be seen from Table 2, the LOI value of pure NR is only 19.1%, which is flammable and cannot pass the test of UL-94. The incorporation of 20 phr ACT resulted in a slight increase

Table 1 Batch compositions

Samples	NR	HD-silica	Si-69	ZnO	CZ	DM	S	N98	APP	ACT
Amount (g)	100	60	10.6	5	2.0	0.6	1	5	Variable	Variable

Table 2 LOI and UL-94 tests experimental data for various samples

Samples	NR (phr)	APP (phr)	Clay (phr)	TA (phr)	LOI (%)	UL-94	Dripping
Neat NR	100	—	—	—	19.1	NC	Yes
NR/APP20	100	20	—	—	20.5	NC	Yes
NR/ACT20	100	14.5	3.67	1.83	22.0	NC	Yes
NR/APP40	100	40	—	—	24.5	V-2	Yes
NR/ACT40	100	29.1	7.27	3.63	28.5	V-1	NO
NR/APP60	100	60	—	—	30.0	V-0	NO
NR/ACT60	100	43.6	10.93	5.47	30.5	V-0	NO

in the LOI value of NR/ACT20 over NR/APP20, but no improvement in the rating of UL-94. With the addition of flame retardants, LOI values and UL-94 grades of composite materials generally showed an upward trend. Compared with the LOI value of 24.5% and UL-94 V-2 grade for the NR/APP40, the NR/ACT40 with LOI value of 28.5% and the UL-94 V-1 grade

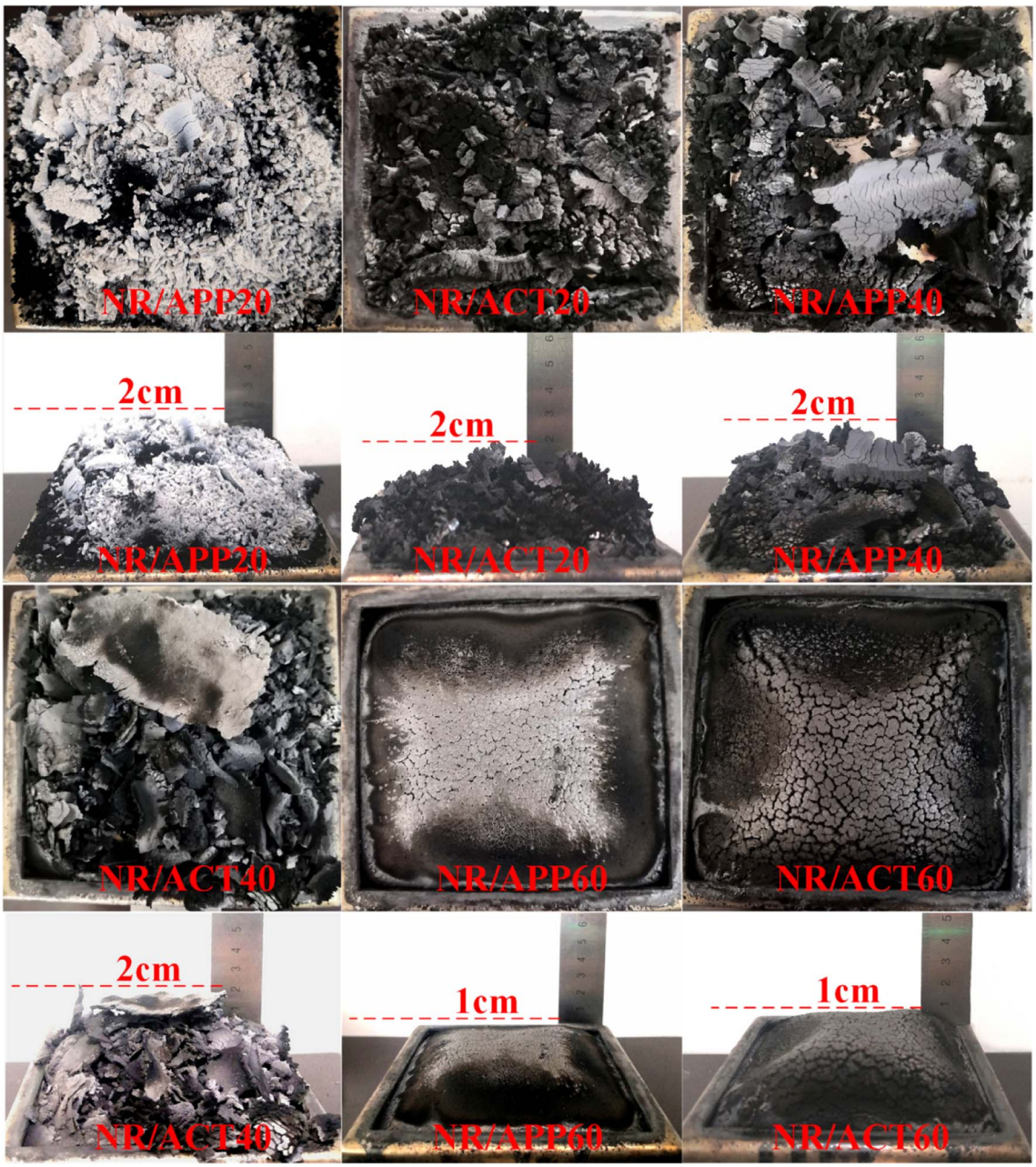

Fig. 1 The char residues digital photos of NR/APP and NR/ACT composites after CCT test.

indicated significantly the improved flame retardant performance. This indicates that an important flame retardant requirement significantly improves the flammability of NR due to its intrinsic fire resistance. NR composites containing 60 phr APP were rated V-0, however, the LOI value of NR/ACT60 with an increase of 1.67% was higher. It is ascribed to the combination of the catalytic carbonization effect of APP originating from metaphosphoric acid (HPO_4) decomposed from APP and the barrier effect of thermostable clay originating from its lamellar microstructure. Digital photos of NR/APP composite carbon residue (Fig. 1) tested by cone calorimeter showed that the carbon residue was compact and strong, but incomplete and did not expand. However, for NR/ACT composites, the char residue is generally dense with high strength. Compared with APP system, ACT system has a much higher amount of carbonization under the same load, indicating that ACT system effectively accelerates the formation of strong char residue in composite materials. Thermal analysis also confirmed this result. TGA and DTG curves of APP and ACT under N_2 atmosphere are shown in Fig. 2, and relevant TGA data are recorded in Table S2.† It can be found that due to the synergistic effect of the three components in the thermal degradation process, there is only one major step for ACT thermal degradation, while APP has three major steps. Compared with APP, the maximum weightlessness temperature (T_{1max}) of ACT is reduced due to TA thermal degradation. However, ACT has higher the initial degradation temperature ($T_{5\%}$, where 5 wt% mass loss takes place in our laboratory) and residues than those of APP. This may be due to the synergistic catalytic charring action of TA, which results in the production of more phosphorus carbon coke slag compared with APP. In addition, the high-aspect-ratio clay can bind the carbon particles together to form a high-strength adiabatic carbon shielding layer on the internal material. The results show that, due to the synergistic flame-retarding mechanism, ACT's flame-retarding effect is significantly higher than APP's.

In order to further study the flame retardant properties of NR/APP and NR/ACT composites, more scientific cone-shaped calorimetry tests were used to evaluate their combustion properties, parameters such as time to ignition (TTI), peak heat release rate (PHRR), total heat release (THR), smoke release rate (RSR), total smoke rate (TSR), total smoke production (TSP) and mass residue after combustion as shown in Fig. 3, and the corresponding data are displayed in Table 3. PHRR and THR are the critical parameters to characterize the fire safety of polymers. In this study, the introduction of APP system or ACT system into pure NR can improve the flame retardancy. In addition, ACT system is more effective than APP system in the performance of NR flame retardant. As shown in Fig. 3(a) and (b), when the heat flux was 35 kW m^{-2}, the HRR and THR peaks of the NR/ACT20 composite were low, which were 473.9 kW m^{-2} and 121.7 mm^{-2}, respectively, while the peak values of the NR/APP20 composite were 659.7 kW m^{-2} and 141.6 mm^{-2}. The PHRR value of the NR/ACT40 composite material decreased by 17.5% compared with that of the NR/APP40 composite material, which showed a significant decrease. With the increase of the amount of flame retardants, the gap between THR and PHRR between APP and ACT systems gradually narrowed. To better understand the fire risk of the two systems studied, the fire performance index (FPI)[27] and the fire growth index (FIGRA)[28] are selected. FPI is defined as the ratio between TTI and PHRR. It is reported that there is a correlation between the material's FPI value and flashover time. When the FPI value is reduced, the flashover time is advanced.[27] Therefore, it can be considered that the smaller the FPI of the material, the higher the fire risk. FIGRA is defined as the ratio of PHRR to HRR peak time. According to previous reports, the greater the FIGRA value, the shorter the time to HRR peak, and the greater the fire risk of the material. The values of FPI and FIGRA of these composites have been shown in Table 3. Compared with APP system, FPI and FIGRA of ACT system greatly improve and reduce the flammability of NR respectively under equivalent loading. Among these composites, the NR/ACT60 has the highest FPI and the lowest FIGRA. The NR/ACT60 shows minimum fire risk. This may be the synergistic effect between APP and TC, resulting in the denser and more phosphor carbon residue produced by NR/ACT (Fig. 3f). The flue gas toxicity of organic materials is the main cause of fire death and injury, so it is of great significance

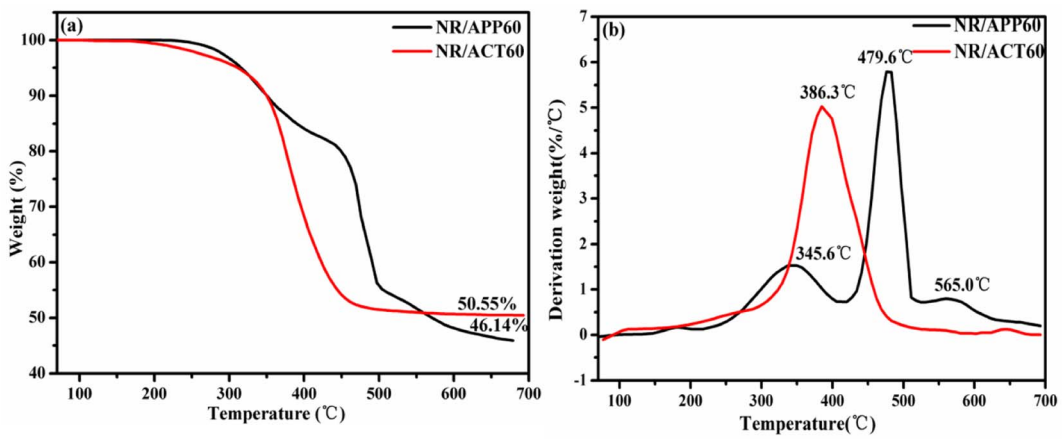

Fig. 2 TGA and DTA thermograms of APP and ACT in N_2 atmosphere.

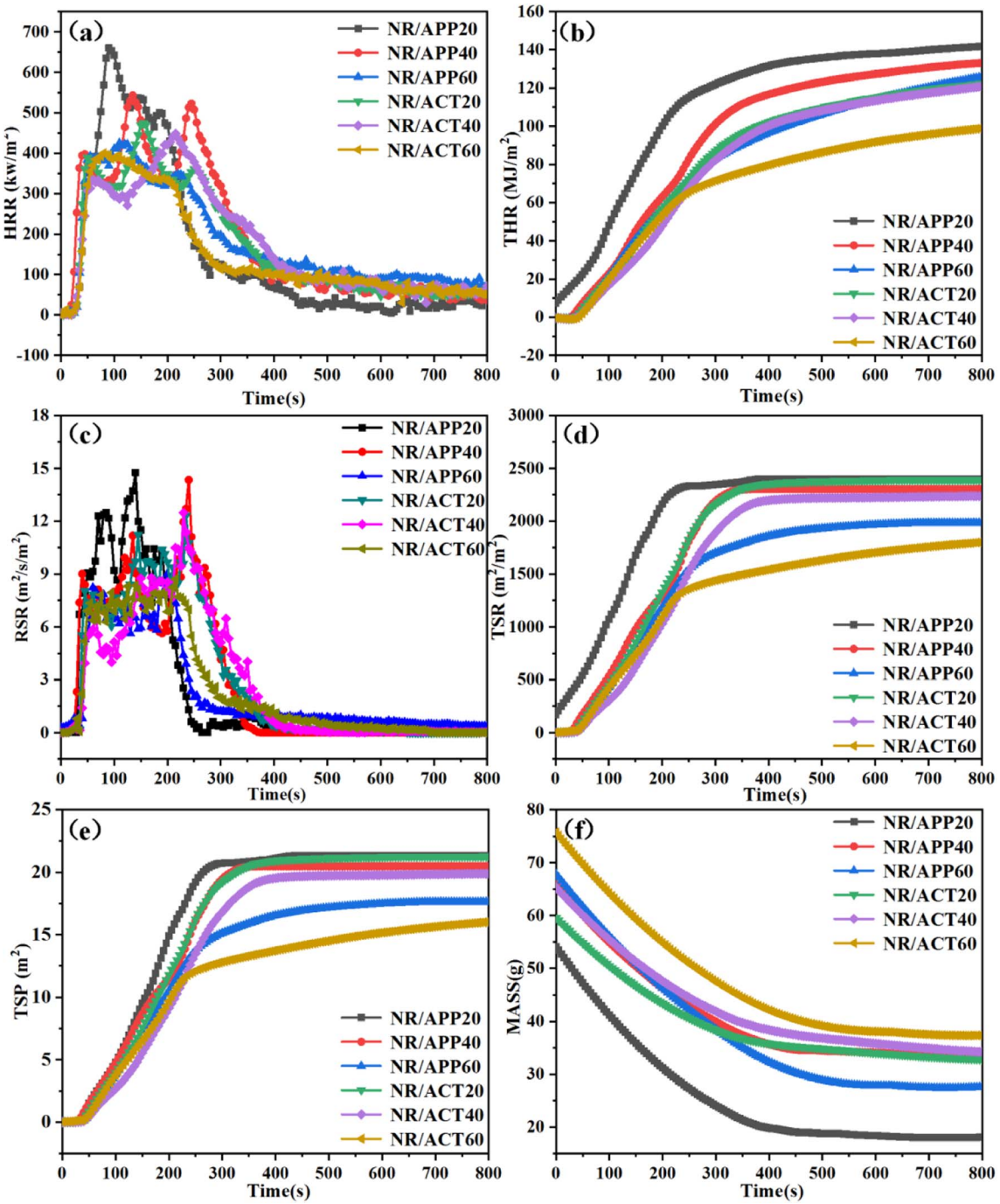

Fig. 3 Combustion properties of NR/APP and NR/ACT composites with an external heat flux of 35 kW m^{-2}: (a) HRR, (b) THR, (c) RSR, (d) TSR, (e) TSP and (f) MASS.

to reduce the flue gas emission during combustion. The dynamic smoke generation behavior of NR/APP and NR/ACT composites was characterized by smoke extraction rate (RSR), total smoke rate (TSR) and total smoke yield (TSP) as shown in Fig. 3(c)–(e), and the data are summarized in Table 3. As can be seen from Fig. 3c, the RSR of NR/ACT composite material is significantly lower than that of NR/APP, and the P-RSR of NR/ACT60 is reduced from 8.32 m^2 s^{-1} m^{-2} to 9.02 m^2 s^{-1} m^{-2}, with a decrease of 7.76%. The reduction of smoke indicates that the ACT flame retardant system can be used as a smoke suppressor to improve the survival rate. Moreover, compared with those of NR/APP composites, TSR (Fig. 3d) and TSP (Fig. 3e) of NR/ACT composites, under the same loading conditions were greatly reduced. The main reason may be that clay acts as a protective barrier to reduce soot transfer and TA's catalytic carbonization and the synergistic effect of clay's carbon layer strengthening. The measured average effective heat comb (EHC) further demonstrate the reduction in flammability due to

Table 3 Cone calorimetry experimental data for various samples

Samples	TTI (s)	PHRR (kW m^{-2})	THR (MJ m^{-2})	TSP (m^2)	MASS (g)	FPI (10^{-2} m^2 s kW^{-1})	FIGRA (kW (m^2 s^{-1})$^{-1}$)	EHC (MJ kg^{-1})
NR/APP20	8	659.7	141.6	21.34	18.10	1.2	7.33	18.95
NR/ACT20	23	473.9	121.7	20.21	32.83	4.9	2.92	11.93
NR/APP40	23	543.2	133.0	20.49	32.98	4.2	3.89	16.41
NR/ACT40	31	448.4	120.9	19.88	34.25	7.3	1.96	19.79
NR/APP60	26	425.2	125.5	17.63	27.58	6.1	3.79	26.52
NR/ACT60	38	400.3	98.8	16.01	37.35	9.5	2.47	33.04

the char formation. So far, the thermal combustion properties of NR/ACT composites have demonstrated the synergistic improvement of thermal stability and flame retardancy. According to the proposed method, the synergistic effect of APP and TC on NR flame retardant treatment was demonstrated and quantified by Lewin[29] and Horrocks *et al.*,[30] and the validity parameter of the synergistic effect (SE) is calculated as shown in the formula Table S3.† SE value greater than 1 is sufficient to represent the collaborative interaction between APP and TC. The results also showed that the amount of flame retardants added had a significant effect on the synergistic activity. Due to the complexity of the rubber formulation system, although the SE value decreases with the increase of flame retardant dosage, the synergistic effect is still significant under the maximum flame retardant dosage.

3.2 Morphology of intumescent char layer

In order to elucidate the effect of coke formation on the combustion of NR composite, the morphology and structure of coke after combustion were studied by scanning electron microscope as shown in Fig. 4.

For the char residue of the NR/APP60 composite, the continuous and compact char layers does not expand, slightly melts and falls, as observed significantly (Fig. 4(a1) and (a3)). It can act as a protective layer on the surface of the internal material and inhibit the transfer of heat and the diffusion of fuel when it comes into contact with flame or heat source. The expanded char residues of the NR/ACT60 composite (Fig. 4(b1) and (b3)) are with a much compacter and denser structure than those of NR/APP due to the synergistic effect of APP and TC. Under high magnification (Fig. 4(a2) and (b2)), Compared

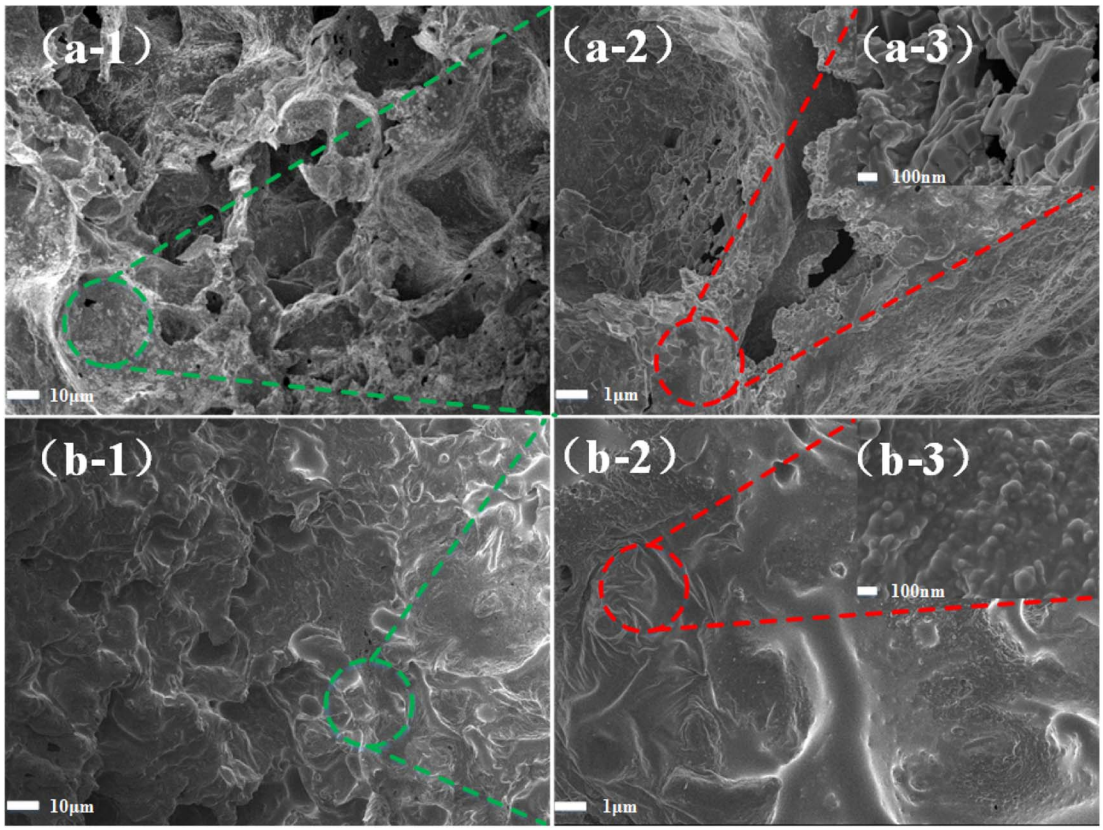

Fig. 4 SEM images of the char residue after CCT test: (a) NR/APP60 and (b) NR/ACT60.

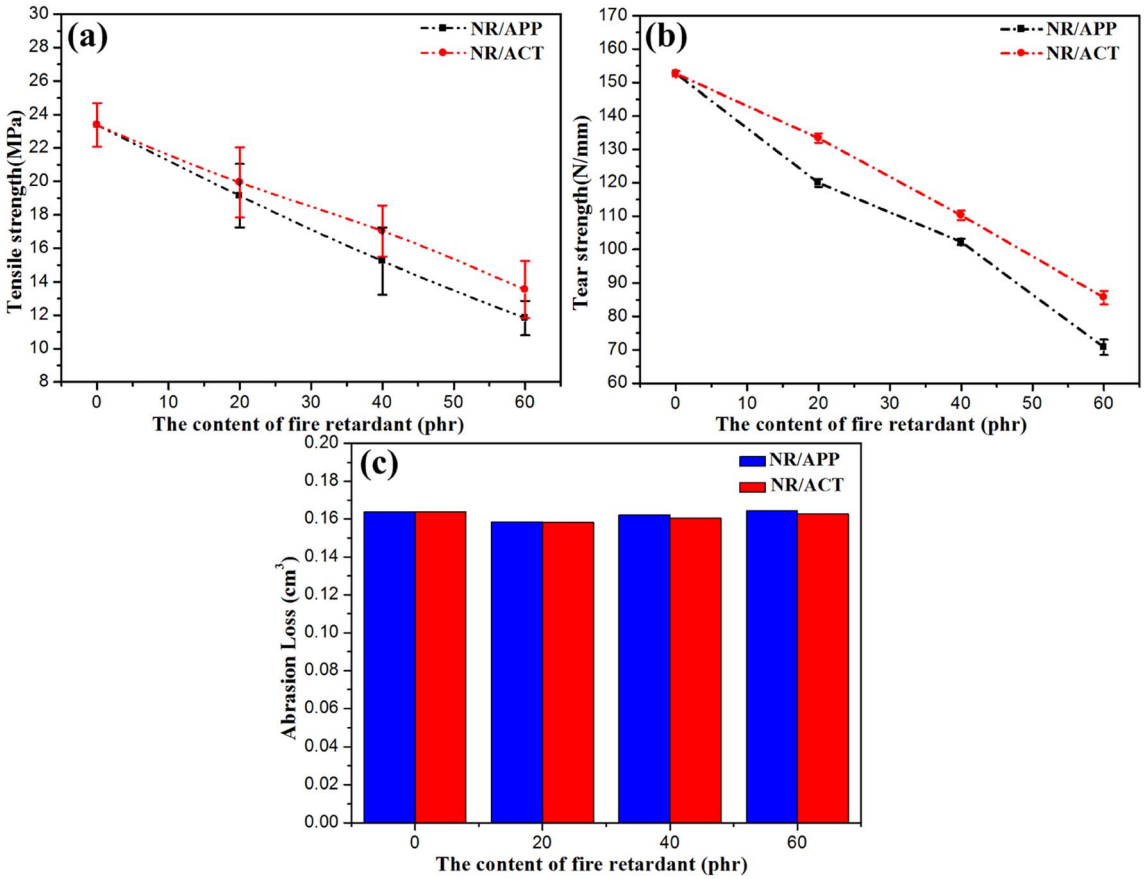

Fig. 5 (a) Tensile strength, (b) tear strength and (c) abrasion loss of NR/APP and NR/ACT composites.

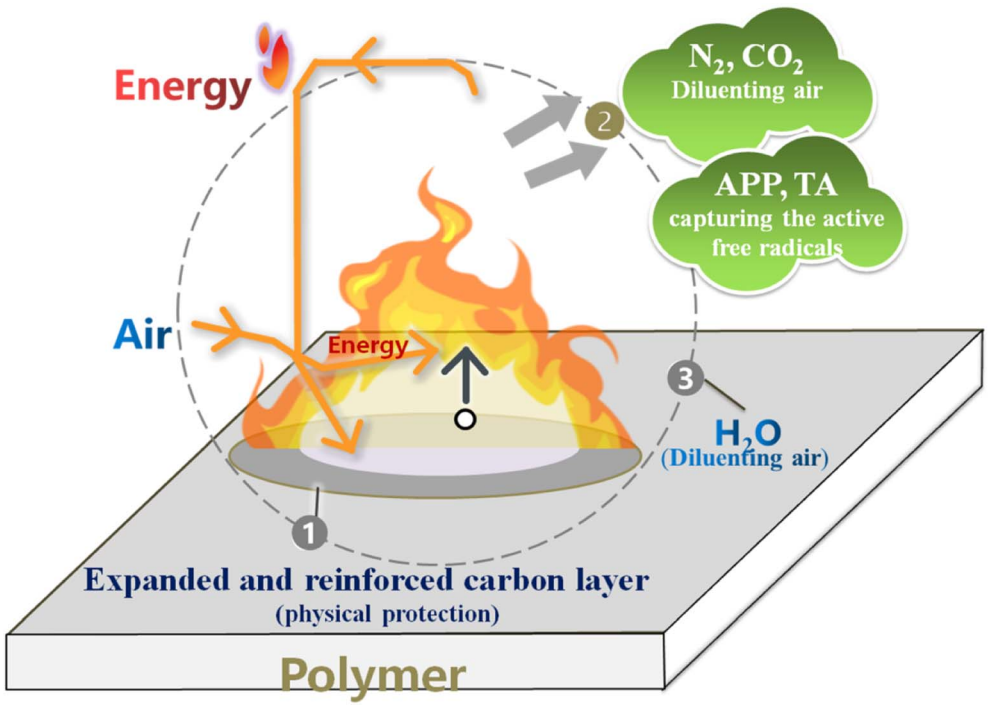

Fig. 6 The flame retarded mechanism scheme of NR/ACT composites.

with NR/APP composite materials, NR/ACT expansive carbon layer is more detailed and complete, which can effectively protect the underlying material from the influence of heat flow or flame, and greatly improve the flame retardant performance of NR composite materials. NR/ACT composites will expand during combustion, and carbonization and extinction will occur immediately after they are released from the fire. Especially for NR/ACT60 char residue at high magnification (Fig. 4(b3)), no defects can be seen due to the formation of sufficiently dense or condensed carbon residue during combustion.

3.3 Mechanical properties of NR/APP and NR/ACT composites

Mechanical properties cannot be ignored for rubber materials. But the mechanical properties of NR could be significantly changed by adding flame retardant. Their flame-retardant effect comes with negative effects, such as pollution of mechanical properties. The polarity difference between polar flame retardants and non-polar NR may be the reason for the poor particle dispersion and interface interaction between polar flame retardants and non-polar NR. With the increase of the amount of APP, the tensile strength and tear strength of NR/APP composites decrease monotonically

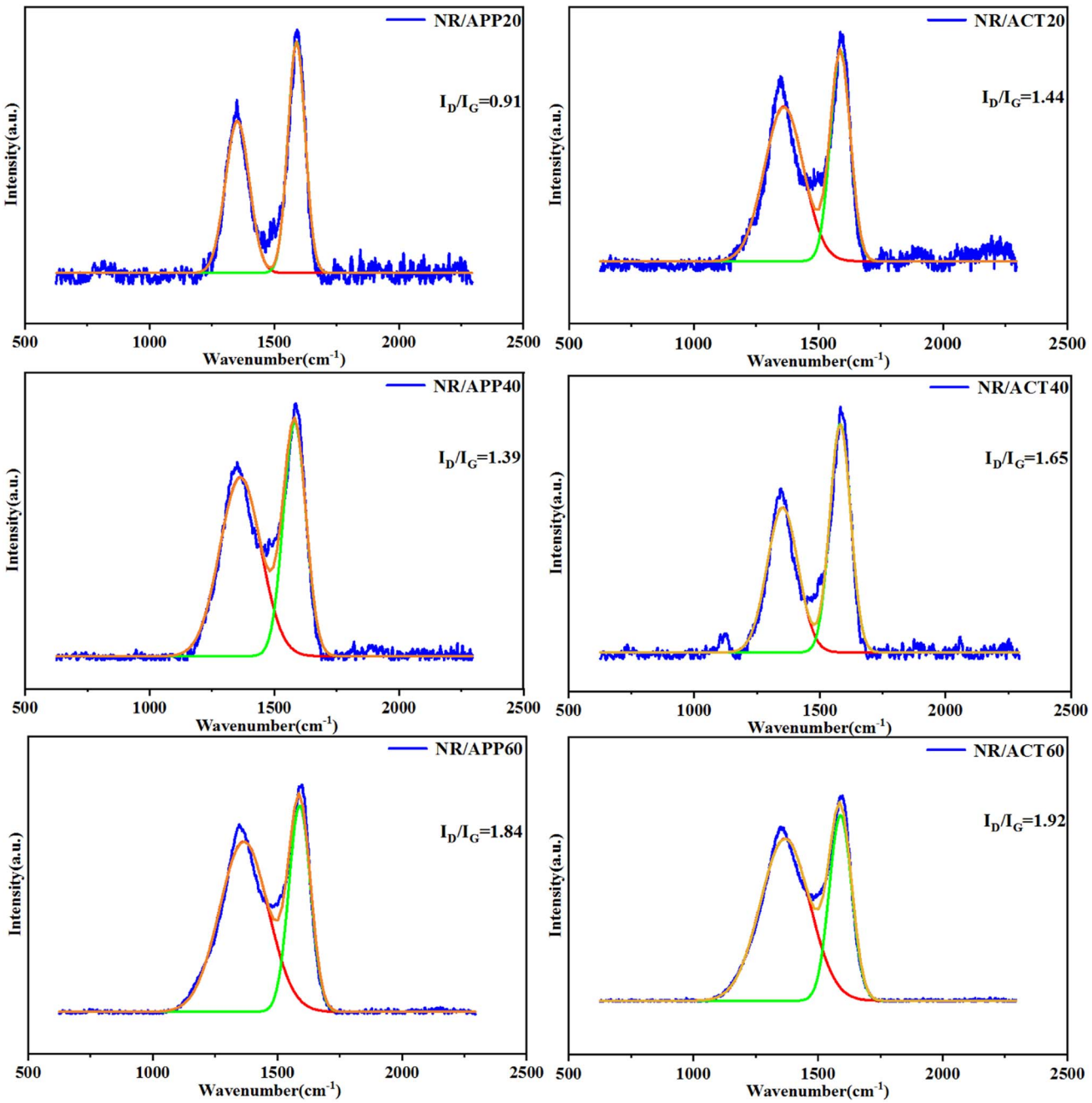

Fig. 7 Raman peak fitting curves of the char residue of composites.

(Fig. 5a and b). Compared with NR/APP composite materials, the abrasion resistance of NR combined with ACT system is significantly improved (Fig. 5c). The tensile strength and tearing strength of NR/ACT composites are superior to that of NR/APP composites. This may be related to the addition of TA in the crosslinking reaction and the enhancement effect of clay on the cross-linking density of natural rubber.[18] This significant improvement was also attributed to the uniform dispersion of TC and the dual effects of dispersant and interfacial regulator of TA, with strong interfacial adhesion between TC and NR.[26,31]

3.4 Flame retardant mechanism

Based on the above analysis, the flame retardant mechanism of ACT system in NR matrix was assumed in Fig. 6. First, for the condensed phase, the heat-stabilized clay sheet acts as a barrier to flammable gas penetration during the early degradation process.[32–35] At the same time, the catalytic charring ability originating from metaphosphoric acid (HPO_4) decomposed from APP and TA results in the formation of phosphocarbon slag. Then the ammonia released by APP is used to inflate the formed carbon layer. Secondly, for the gas phase, the volatile products in the combustion process can effectively diluted by the ammonia released by APP. It can be seen that the tripartite synergistic mechanism for ACT system mainly contributes to the excellent flame-retardant performance of NR composites. The chemical structure of char residue is confirmed by Raman spectrometer. As shown in Fig. 7, the curve fitting software Originpro 2017/Peak Fitting Module was used to perform peak fitting for each spectrum and analyze the curve into the 2 Gian band (Fig. 7). Typically, the combined strength (I_D/I_G) of the D to G bands reflects the degree of graphitization of the carbon residue.[36] Basically, the bigger ratio of I_D/I_G is, the smaller size of carbonaceous microstructures is, and the denser the microstructure is.[37–39] It is worth noting that under the same loading conditions, the I_D/I_G ratio always follows the NR/ACT > NR/APP sequence, indicating that the ACT system can make the pulverized coal structure more compact and effectively improve the flame retardancy, which is the main reason for the inhibition of flammability.

4 Conclusion

In this study, the new ACT flame retardant has synergistic flame retardant and smoke suppression effect on NR due to its expansion flame retardant mechanism. Raman spectroscopy and SEM analysis of the char residue showed that the ACT system could significantly promote the formation of carbon layers with high graphitization and phosphorous structure, thus effectively reducing the combustion performance parameters and fire risk. Moreover, the ACT system is conducive to the mechanical properties of NR with the appropriate amount of addition, even though, under high loading conditions, the ACT system has much less damage to the mechanical properties of NR than the APP system under the same loading conditions.

Conflicts of interest

There are no conflicts to declare.

Acknowledgements

Financial support from projects funded by Natural Science Foundation of China (51703111 and 51603111), Natural Science Foundation of Shandong Province (ZR2021ME107) and project funded by China Postdoctoral Science Foundation (2021M700553 and 2020M672014) are gratefully acknowledged.

References

1 F. Laoutid, L. Bonnaud, M. Alexandre, J. M. Lopez-Cuesta and P. Dubois, New prospects in flame retardant polymer materials: from fundamentals to nanocomposites, *Mater. Sci. Eng., R*, 2009, **63**(3), 100–125.
2 S. Bourbigot, M. L. Bras, S. Duquesne and M. Rochery, Recent advances for intumescent polymers, *Macromol. Mater. Eng.*, 2004, **289**, 499–511.
3 G. Bai, C. Guo and L. Li, Synergistic effect of intumescent flame retardant and expandable graphite on mechanical and flame-retardant properties of wood flour-polypropylene composites, *Constr. Build. Mater.*, 2014, **50**, 148–153.
4 S. Y. Lee, K. M. Kim, D. G. Seong and D. J. Lee, Synergistic improvement of flame retardant properties of expandable graphite and multi-walled carbon nanotube reinforced intumescent polyketone nanocomposites, *Carbon*, 2019, **143**, 650–659.
5 K. S. Lim, S. T. Bee, L. T. Sin, T. T. Tee, C. T. Ratnam, D. Hui and A. R. Rahmat, A review of application of ammonium polyphosphate as intumescent flame retardant in thermoplastic composites, *Composites, Part B*, 2016, **84**, 155–174.
6 X. F. Chen, C. Y. Huang, Y. Q. Shi, B. H. Yuan, Y. R. Suna and Z. M. Bai, MoO_3-ZrO_2 solid acid for enhancement in the efficiency of intumescent flame retardant, *Powder Technol.*, 2019, **344**, 581–589.
7 B. H. Yuan, Y. Hu, X. F. Chen, Y. Q. Shi, Y. Niu, Y. Zhang, S. He and H. M. Dai, Dual modification of graphene by polymeric flame retardant and $Ni(OH)_2$ nanosheets for improving flame retardancy of polypropylene, *Composites, Part A*, 2017, **100**, 106–117.
8 Y. W. Yan, L. Chen, R. K. Jian, S. Kong and Y. Z. Wang, Intumescence: an effect way to flame retardance and smoke suppression for polystyrene, *Polym. Degrad. Stab.*, 2012, **97**, 1423–1431.
9 F. Fang, D. Z. Xiao, X. Zhang, Y. D. Meng, C. Cheng, C. Bao, X. Ding, H. Cao and X. Y. Tian, Construction of intumescent flame retardant and antimicrobial coating on cotton fabric via layer-by-layer assembly technology, *Surf. Coat. Technol.*, 2015, **276**, 726–734.
10 L. Wang, W. Yang, B. B. Wang, Y. Wu, Y. Hu, L. Song and K. K. Yuen, The impact of metal oxides on the combustion behavior of ethylene-vinyl acetate copolymers containing

an intumescent flame retardant, *Ind. Eng. Chem. Res.*, 2012, **51**, 7884–7890.

11 P. Wen, D. Wang, J. Liu, J. Zhan, Y. Hu and R. K. K. Yuen, Organically modified montmorillonite as a synergist for intumescent flame retardant against the flammable polypropylene, *Polym. Adv. Technol.*, 2017, **28**, 679–685.

12 S. Elbasuney, Novel multi-component flame retardant system based on nanoscopic aluminium-trihydroxide (ATH), *Powder Technol.*, 2017, **305**, 538–545.

13 Z. M. Zhu, L. X. Wang and L. P. Dong, Influence of a novel P/N-containing oligomer on flame retardancy and thermal degradation of intumescent flame-retardant epoxy resin, *Polym. Degrad. Stab.*, 2019, **162**, 129–137.

14 G. B. Huang, S. Q. Wang, P. A. Song, C. L. Wu, S. Q. Chen and X. Wang, Combination effect of carbon nanotubes with graphene on intumescent flame-retardant polypropylene nanocomposites, *Composites, Part A*, 2014, **59**, 18–25.

15 S. Lee, H. M. Kim, D. G. Seong and D. Lee, Synergistic improvement of flame retardant properties of expandable graphite and multi-walled carbon nanotube reinforced intumescent polyketone nanocomposites, *Carbon*, 2019, **143**, 650–659.

16 M. Li and J. Shi, Review on micropore grade inorganic porous medium based form stable composite phase change materials: Preparation, performance improvement and effects on the properties of cement mortar, *Constr. Build. Mater.*, 2019, **194**, 287–310.

17 P. Alisa, I. Kamonnart and O. Makoto, Designing nanoarchitecture for environmental remediation based on the clay minerals as building block, *J. Hazard. Mater.*, 2020, **399**, 122888–122925.

18 S. Zhao, S. C. Xie, Z. Zhao, J. L. Zhang, L. Li and Z. X. Xin, Green and high-efficiency production of graphene by tannic acid assisted exfoliation of graphite in water, *ACS Sustainable Chem. Eng.*, 2018, **6**, 7652–7661.

19 M. B. Ma, S. Z. Dong, M. Hussain and W. L. Zhou, Effects of addition of condensed tannin on the structure and properties of silk fibroin film, *Polym. Int.*, 2017, **66**, 151–159.

20 Y. Takashi, H. Tsutomu and I. Hideyuki, Chapter seven-high molecular weight plant polyphenols (tannins): Prospective Functions, *Recent Adv. Phytochem.*, 2005, **39**, 163–190.

21 F. Alihosseini and G. Sun, 17-Antibacterial colorants for textiles, *Woodhead Publ. Ser. Text.*, 2011, **18**(9), 376–403.

22 B. Adamczyk, J. P. Salminen, A. Smolander and V. Kitunen, Precipitation of proteins by tannins: effects of concentration, protein/tannin ratio and Ph, *Int. J. Food Sci. Technol.*, 2012, **47**, 875–878.

23 R. Majumdar, B. G. Bag and P. Ghosh, Mimusops elengi bark extract mediated green synthesis of gold nanoparticles and study of its catalytic activity, *Appl. Nanosci.*, 2016, **6**, 521–528.

24 H. Tributsch and S. Fiechter, The material strategy of fire-resistant tree barks, in *High Performance Structures and Materials IV*, ed. W. P. De Wilde and C. A. Brebbia, WIT Press, 2008, pp. 43–52.

25 L. Lin, *et al.*, Synergistic effects of a highly effective intumescent flame retardant based on tannic acid functionalized graphene on the flame retardancy and smoke suppression properties of natural rubber, *Composites, Part A*, 2020, **129**, 105715.

26 L. Li, J. Zhang, J. O. Jo, S. Datta and J. K. Kim, Effects of variation of oil and zinc oxide type on the gas barrier and mechanical properties of chlorobutyl rubber/epoxidized natural rubber blends, *Mater. Des.*, 2013, **49**, 922–928.

27 Z. B. Shao, C. Deng, Y. Tan, L. Yu and M. J. Chen, Ammonium polyphosphate chemically-modified with ethanolamine as an efficient intumescent flame retardant for polypropylene, *J. Mater. Chem. A*, 2014, **2**, 13955–13965.

28 J. N. Wu, L. Chen, T. Fu, H. B. Zhao, D. M. Guo, X. L. Wang and Y. Z. Wang, New application for aromatic Schiff base: high efficient flame-retardant and anti-dripping action for polyesters, *Chem. Eng. J.*, 2018, **336**(15), 622–632.

29 M. Lewin, Synergism and catalysis in flame retardancy of polymers, *Polym. Adv. Technol.*, 2001, **12**, 215–222.

30 A. R. Horrocks, G. Smart, S. Nazaré, B. Kandola and D. Price, Quantification of zinc hydroxystannate and stannate synergies in halogen-containing flame-retardant polymeric formulations, *J. Fire Sci.*, 2010, **28**(3), 217–248.

31 Y. Gao, L. Q. Liu, S. Z. Zu, K. Peng, D. Zhou, B. H. Han and Z. Zhang, The effect of interlayer adhesion on the mechanical behaviors of macroscopic graphene oxide papers, *ACS Nano*, 2011, **5**(3), 2134–2141.

32 D. Zhao, J. Wang, X. L. Wang and Y. Z. Wang, Highly thermostable and durably flame-retardant unsaturated polyester modified by a novel polymeric flame retardant containing Schiff base and spirocyclic structures, *Chem. Eng. J.*, 2018, **344**, 419–430.

33 P. Khalili, X. L. Liu, Y. T. Kim, C. Rudd, X. S. Yi and I. Kong, Development of fire retardancy of natural fiber composite encouraged by a synergy between zinc borate and ammonium polyphosphate, *Composites, Part B*, 2019, **159**, 165–172.

34 O. Das, N. K. Kim, M. S. Hedenqvist and D. Bhattacharyya, The flammability of biocomposites, in *Durability and life prediction in biocomposites, fibre-reinforced composites and hybrid composites*, Woodhead Publishing. 2019; pp. 335–365.

35 T. Perroud, V. Shanmugam, R. A. Mensah, L. Jiang, Q. Xu, R. E. Neisiany, G. Sas, M. Forsth, N. K. Kim and M. S. Hedenqvist, Testing bioplastics containing functionalised biochar, *Polym. Test.*, 2022, 107657.

36 X. Feng, X. Wang, W. Cai, S. Qiu, Y. Hu and K. M. Liew, Studies on synthesis of electrochemical exfoliated functionalized graphene and polylactic acid/f-GNS nanocomposites as new fire hazard suppression materials, *ACS Appl. Mater. Interfaces*, 2016, **8**, 25552–25562.

37 S. Bourbigot, M. Le Bras, R. Delobel, R. Decressain and J. P. Amoureux, Synergistic effect of zeolite in an

intumescence process: study of the carbonaceous structures using solid-state NMR, *J. Chem. Soc., Faraday Trans.*, 1996, **92**, 149–158.

38 S. Hu, L. Song, H. F. Pan and Y. Hu, Thermal properties and combustion behaviors of chitosan based flame retardant combining phosphorus and nickel, *Ind. Eng. Chem. Res.*, 2012, **51**(9), 3663–3669.

39 L. Song, K. Wu, Y. Wang, Z. Wang and Y. Hu, Flammability and thermo-oxidative decomposition of epoxy resin containing ammonium polyphosphate and metallic oxide, *J. Macromol. Sci., Part A: Pure Appl.Chem.*, 2009, **46**(3), 290–295.